VALIDATING EMERGING TRANSMISSION TECHNOLOGIES ON SUBMARINE CABLE SYSTEMS

Priyanth Mehta, Andrzej Borowiec, Charles Laperle, Sandra Feldman, and Michael Reimer (Ciena)
Email: prmehta@ciena.com

Ciena, 385 Terry Fox Dr, Ottawa, ON K2K 0L1.

Abstract: Transponder technologies are continually being developed with enhanced feature sets from multi-dimensional modulations to sub-carrier multiplexed probabilistically shaped constellations. In the transition between generations of product development, an extensive simulation and experimental study is completed to determine the performance impact for a new ASIC feature. Experimental validations are typically performed offline using capture-and-compute hardware in the lab or in the field on in-service cable systems. The simulators are ideally used to drive the transmit DAC waveforms and perform recovery on the waveforms captured by the ADCs in the receiver. However, the type of hardware and simulators employed can have dramatic effects on the results that aren't necessarily demonstrated to the same degree in real-time technologies. This paper describes the accuracy of offline technologies compared to real-time product performance. Finally, capture-and-compute systems are used in the field to demonstrate near term ASIC features improving system capacity through dry technology enhancements.

1. INTRODUCTION

Real-time coherent transmission technologies require a digital backend and analogue frontend. The digital component is driven by the ASIC, whereas the analogue components consist of DACs, ADCs, and electro-optic devices. **Figure 1** and **Figure 2** are high-level examples of coherent transmitters and receivers.

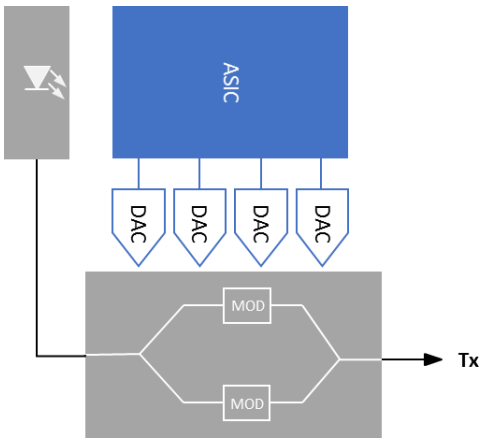

Figure 1. Real-time coherent transmitter.

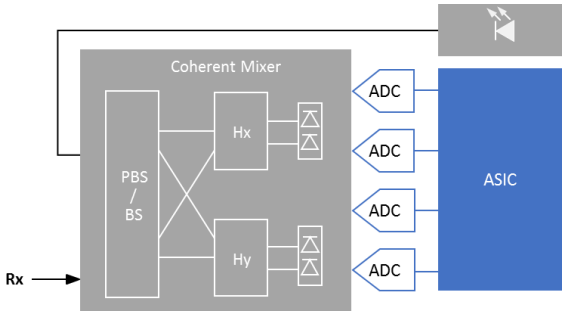

Figure 2. Real-time coherent receiver.

In these examples, the electro-optic components stay relatively static in design and typically mature for higher bandwidth requirements. The ASICs however encompass a large array of features responsible for the digital signal processing (DSP) of the generated and sampled optical fields. Advancements in CMOS feature sizes support larger and more complex DSP computations that can be integrated in the ASIC. Before CMOS integration can be achieved, DSP features are simulated over distributed computing resources to evaluate feature performance.

Offline capture-and-compute systems are a simplified means for testing these ASIC features experimentally.

2. METHOD

Figure 3 is an example of an offline transmitter where the ASIC is replaced by a PC or offline DSP and the DACs are provided by an arbitrary waveform generator (AWG). The offline DSP generates an analogue waveform with the symbols encoded using the designed DSP feature set. The waveform is loaded into the AWG which drives the electro-optical modulator to generate an optical signal.

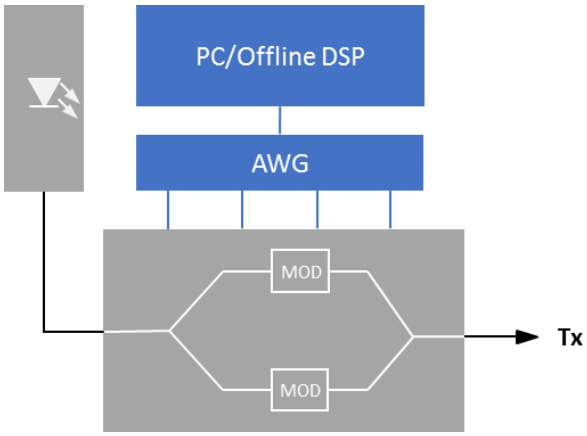

Figure 3. Offline transmitter.

Figure 4 is an example of an offline receiver. The optical signal from the coherent mixer is received by a real-time sampling oscilloscope which replaces the ADCs of **Figure 2**. The PC captures the waveform from the sampling scope, and processing of the field occurs in the DSP simulator.

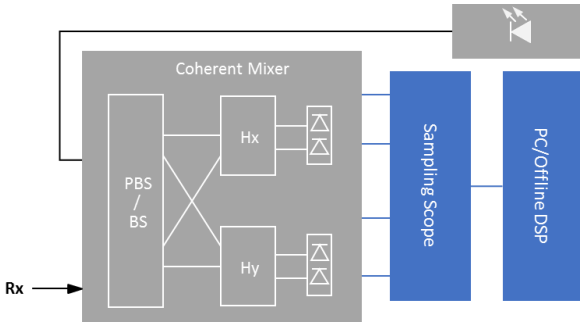

Figure 4. Offline receiver.

In the very early stages of transceiver development, the simulator used to generate and process the transmit and receive waveforms uses high precision floating point calculations. The calculations may not necessarily perform blind recovery on the received symbols, but carrier recovery can be assisted by cross-correlation of the received symbols with the transmit symbols. This can often result in optimistic performance. Furthermore, real-time ASICs are limited by finite-length digital time domain filters and are constrained to fixed point arithmetic [1]. For this reason, signal processing algorithms and error correction logic are specified with bit exact models in high level languages such as C and then converted to a register transfer language (RTL). The RTL description is broken down into smaller logic entities, as multiplexers, adders, flip-flops, or basic logic functions [2] to form the ASIC.

Recovery of the captured waveforms through floating point or fixed point simulators yields an SNR. The margin is determined by the difference between this SNR and the Required SNR (RSNR) of the line rate or modulation format of interest. RSNRs are typically calculated through independent FEC simulators that produce a bit error rate threshold. The type of FEC simulated can have a wide array of net coding gains [3]; only FEC designs that are implementable in the near term are considered. The BER is attained by a Monte-Carlo simulation of the transmission format with a PRBS sequence. A pre-defined amount of noise is added to degrade the SNR of the PRBS. Hard decision detection is used on the noise loaded PRBS to identify bit errors, forming a relationship between SNR and BER. The $RSNR$ of the system is the SNR due to ASE noise (SNR_{ase}) required to achieve the FEC BER limit.

Capture and compute activities begin in the lab. An attempt is made to achieve system implementation and distortion penalties which align as closely as possible to the intended product specification. The penalties are measured through a process of optical

noise loading. The ASE and recovered receive SNR are used in a fit to:

$$\frac{1}{SNR} = \delta\left(\frac{1}{SNR_{ase}} + \frac{1}{SNR_m}\right)$$

Where δ is the distortion and SNR_m is the implementation SNR. Many factors such as amplitude response, phase response, DAC and ADC dynamic range, etc can affect δ and SNR_m.

In the absence of straight line testbeds, field cable systems are an ideal environment particularly in the presence of foreign waves. The capture and compute system generate an optical field that is highly correlated with its real-time equivalent thereby introducing a comparable nonlinear noise. Back-to-back and field propagated performance is evaluated for next generation transceivers under both floating point and fixed point arithmetic. The digital recovery process of the received optical signal is shown in **Figure 5**.

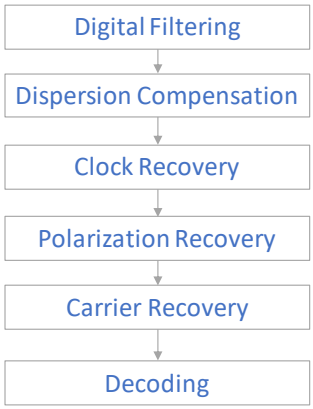

Figure 5. Block diagram of receiver recovery.

It is important to note that fixed point C-based simulators can take hours to evaluate an SNR through blind recovery whereas floating point recovery can be significantly faster. Floating point calculations are therefore used as an indicator of signal quality which determine the valid waveforms to be used in more accurate product simulators.

3. RESULTS AND DISCUSSION

Technology Validation

A 400G geometrically shaped modulation is used to generate a high cardinality format to stress the capture and compute system. The signal is processed as described in **Figure 6** where the difference between the local oscillator (LO) and the transmit laser frequency known as the intermediate frequency (IF) is established.

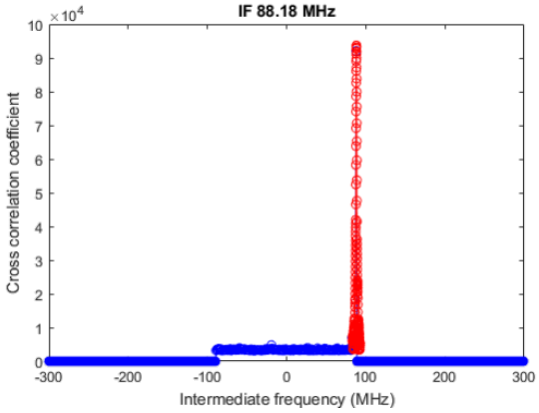

Figure 6. Intermediate frequency estimation for carrier recovery.

Figure 7 shows the IF, followed by a 2x2 multiple input, multiple output (MIMO) filter for polarization recovery.

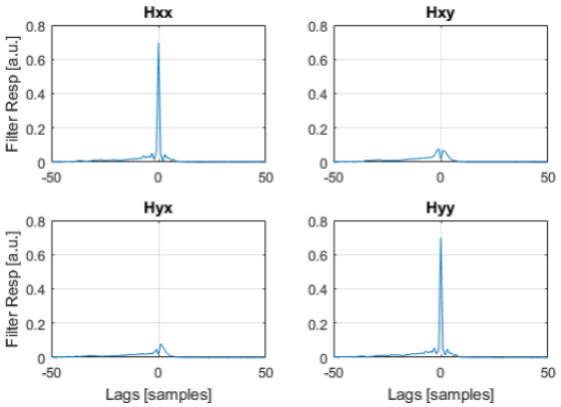

Figure 7. 2x2 MIMO for polarization recovery.

Finally, the receive symbols are decoded and shown in **Figure 8**. Since the transmit symbols is known, an accurate SNR is determined by subtracting the receive constellation from the transmit to calculate the noise power. From the SNR, the BER is

extracted using the aforementioned Monte-Carlo results.

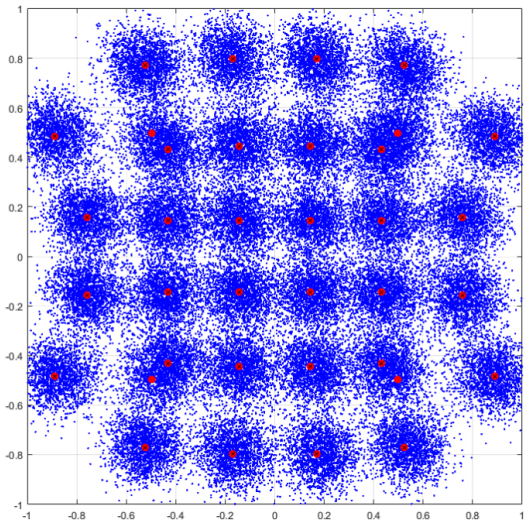

Figure 8. Decoded 400G constellation.

Both floating and fixed point recovery simulators are used to determine the Q margin as a function of OSNR for the 400G signal. The two simulators yield largely different results as seen in **Figure 9**. It is typically expected that floating point precision would yield significantly better performance as it isn't subject to finite filter lengths, DSP taps, fixed point algorithmic noise, and quantization noise.

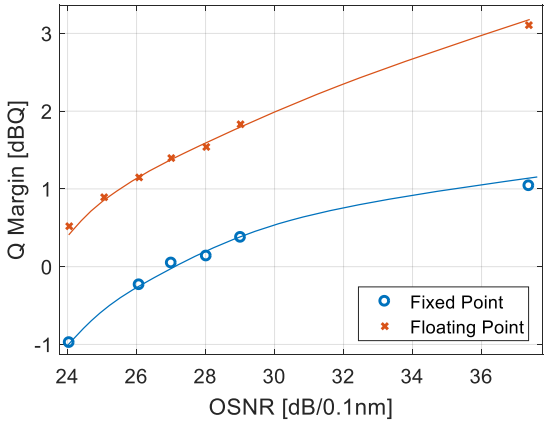

Figure 9. Comparison of offline simulators.

For complex experiments such as tolerance to neighbouring channel cross-talk, three 400G waves were arranged in a back-to-back configuration using offline transmitters. The grid spacing was varied from 56 GHz to 75 GHz and a received Q factor was determined. The recovery was processed with a C-based ASIC simulator that formed the RTL of the real-time WaveLogic AI product. **Figure 10** shows the result of the offline capture and compute cross-talk experiment, along with the same measurement repeated with a Ciena WaveLogic AI modem. The two data sets demonstrate good agreement with a slightly optimistic performance in the offline system. This difference can be attributed to non-idealities in the product's analogue response functions or environmental factors such as thermal and vibrational effects which aren't considered in the simulator.

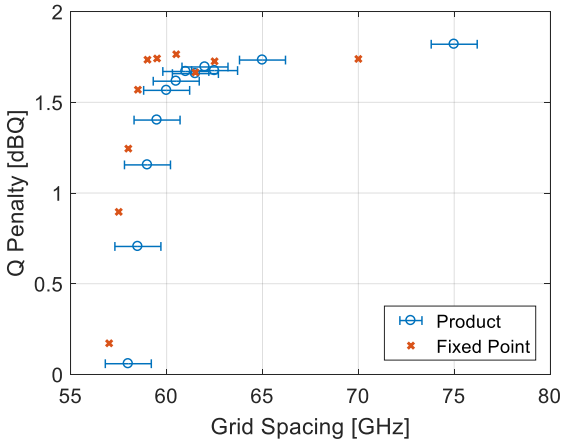

Figure 10. Product vs fixed point offline recovery.

Emerging Technologies

The emergence of higher RF bandwidth drivers, DACs, and ADCs provides a base to explore higher baud transmission technologies. After the offline capture and compute system has achieved a desirable back-to-back performance, field testing of next generation ASIC features can be conducted. In the prototype, advanced technology features were field tested over two dispersion uncompensated cable systems. 16QAM and 64QAM probabilistic shaped constellations (PCS) at 71.3GBd were generated. The client rates varied from 200G to 600G over four frequency division

multiplexed (FDM) carriers. An FDM approach helps mitigate the laser frequency noise associated with very high dispersion systems [4].

When the waveform is generated and uploaded to the transmit DAC, the transmit spectrum and constellation in **Figure *11*** is produced.

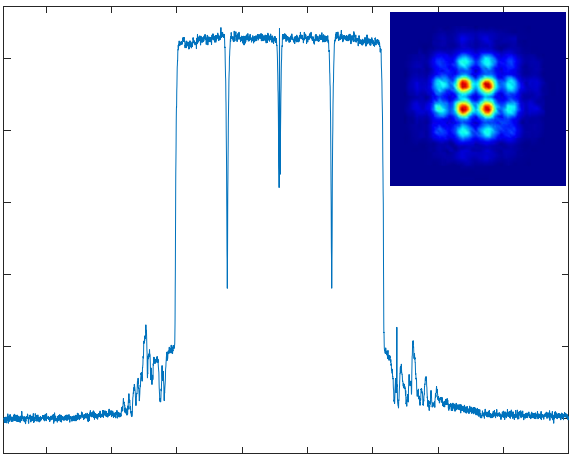

Figure 11. Four FDM transmit spectrum encoded with PCS.

An 8,400km trans-Pacific cable system was tested across 4.5THz of spectrum for performance of the 71.3GBd signal on a 75GHz grid spacing. The system specifications are shown in **Table *1***. Waveform captures were taken at the end of the link and processed. The processing of all field results use a full ASIC simulator. The results of the typical Q margin across the band for each client rate is shown in **Figure *12***.

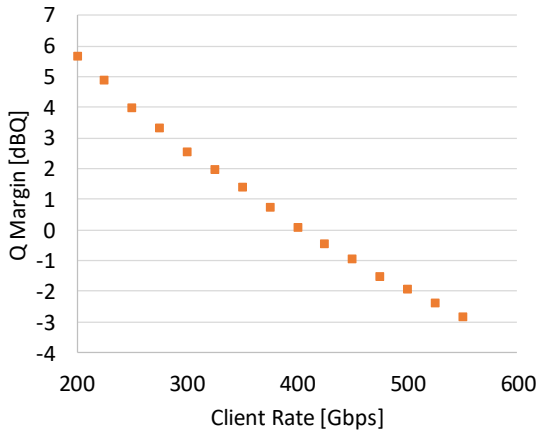

Figure 12. Q Margin over an 8,400km field cable system.

The results demonstrate 400G running with positive margin and a spectral efficiency of 5.33b/s/Hz. This indicates that over the 4.5THz of optical bandwidth, the 8,400km link has a potential of 24Tbps per fibre.

In another instance with the same transmitter features, a 20,300km cable system without optical to electrical regeneration was tested at an 87.5GHz grid spacing. The specifications of the field system are shown in **Table 1. Description of field system parameters.**

	8,400km	**20,300km**
Spans	145	336
TOP [dBm]	17	18
Repeater Bandwidth [nm]	35.4	34.3
OSNR at Pfib [dB/0.1nm]	20	18

Table 1. Description of field system parameters.

The results of the 20,300km are shown in **Figure 13** where 300G operates with ~0.5dBQ of margin, yielding a spectral efficiency of 3.43b/s/Hz. The spectral efficiency distance product of 3.43 x 20300 = 68,600b/s/Hz-km beats all previous records [5].

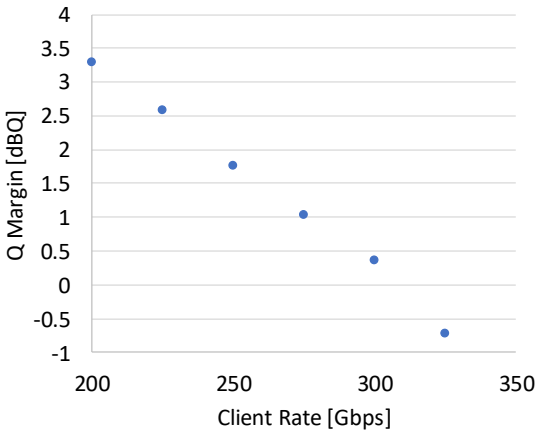

Figure 13. Q Margin over a 20,300km field cable system.

4. CONCLUSION

Capture and compute systems can be variable in performance speculations depending on the simulators used. Fixed point simulators provide the best match as a real-time performance indicator. The simulators used were also tested in the field on different reach cable systems. In all cases, the generated waveforms were captured over the respective links and performance predictions demonstrate PCS and FDM as promising candidates for next generation transmission technologies.

5. REFERENCES

[1] T Sherborne, B Banks, D Semrau, R I Killey, P Bayvel and D Lavery, On the Impact of Fixed Point Hardware for Optical Fiber Nonlinearity Compensation Algorithms, J. Lightwave Technology, Vol 36, No 20, 2018.

[2] A Leven, and L Schmalen, Implementation Aspects of Coherent Transmit and Receive Functions in Application-Specific Integrated Circuits, OFT VI, Vol A, 6th edition.

[3] K Roberts, Q Zhuge, I Monga, S Gareau, and C Laperle, Beyond 100 Gb/s: Capacity, Flexibility and Network Optimization, J. Opt. Commun. Netw., vol. 9, no. 4, pp. C12-C24, Apr. 2017.

[4] A Kakkar, J R Navarro, R Schatz, X Pang, O Ozolins, A Udalcovs, H Louchet, and S Popov, G Jacobsen, Laser Frequency Noise in Coherent Optical Systems: Spectral Regimes and Impairments, Scientific Reports, vol 7, no. 844, Apr. 2017.

[5] V Kamalov, L Jovanovski, V Vusirikala, S Zhang, F Yaman, K Nakamura, T Inoue, E Mateo, and Y Inada, Evolution from 8QAM live traffic to PS 64-QAM with Neural-Network Based Nonlinearity Compensation on 11000 km Open Subsea Cable, OFC/NFOEC 2018, Th4D.5.